Asian Journal of Chemistry; Vol. 38, No. 8 (2026), 2215-2224
ASIAN JOURNAL OF CHEMISTRY
https://doi.org/10.14233/ajchem.2026.36504

Green Synthesis, Bioevaluation and Molecular Docking Studies of a Novel Sulphone-Derived Schiff Base Ligand and its Metal(II) Complexes

C. KRISHNA MOORTHY[1], T. GOMATHI[2], M. KANNAN[3] and T. MOHANAPRIYA[4,*]

[1]Department of Chemistry, Kangeyam Institute of Technology, Kangeyam, Tirupur-638108, India
[2]Department of Chemistry, Paavai College of Engineering, Namakkal-637018, India
[3]Department of Bioinformatics, Saveetha School of Engineering, Saveetha Institute of Medical and Technical Sciences, Saveetha University, Chennai-602105, India
[4]Department of Chemistry, Erode Arts and Science College (Autonomous), Erode-638009, India

*Corresponding author: E-mail: mohanapriyat239@gmail.com

Received: 24 May 2026 *Accepted*: 31 July 2026 *Published online*: 7 August 2026 AJC-22450

A Schiff base ligand was synthesised *via* the condensation reaction of 4,4′-sulfonyldianiline and furfuraldehyde using cashew nut shell liquid (CNSL)-derived anacardic acid, which served as an environmentally benign and naturally efficient catalyst under solvent-free conditions**.** The resulting Schiff base was subsequently reacted with Co(II), Ni(II), Cu(II) and Zn(II) acetate precursors to produce the corresponding metal complexes. The widespread utilisation of organic solvents poses a significant environmental concern because of the generation of hazardous byproducts. The increasing focus on sustainable synthetic methodologies has accelerated the use of solvent-free green catalytic systems as an attractive alternative to conventional protocols. These methods reduce solvent usage, limit waste generation and improve process sustainability. The structural and coordination characteristics of the synthesised ligand and its metal complexes were established using UV-Visible, FT-IR, ^{1}H NMR, ^{13}C NMR, mass spectrometry and scanning electron microscopy (SEM). The synthesized ligand and its metal complexes were evaluated for antimicrobial activity against *E. coli*, *S. aureus* and *C. albicans* using the agar well diffusion method. The tested compounds exhibited appreciable antimicrobial activity against the selected microorganisms. The Schiff base ligand and its Cu(II) complex were further assessed for cytotoxicity against the MCF-7 human breast cancer cell line using the MTT assay. Molecular docking of the Cu(II) complex with the HER2 receptor revealed favourable binding interactions, supporting its potential biological significance.

Keywords: Cashew nut shell liquid (CNSL), MCF-7, Molecular docking, Ligand–protein.

INTRODUCTION

Green catalytic systems have become an important focus in synthetic chemistry because they reduce waste generation, minimize energy consumption and avoid the use of hazardous reagents. Natural acid catalysts are particularly attractive owing to their mild acidity, environmental compatibility, enzymatic characteristics, low cost and ability to promote reactions under ambient conditions [1,2]. Among renewable resources, cashew nut shell liquid (CNSL), an abundant agricultural by-product, has emerged as a valuable feedstock for sustainable chemical synthesis. Anacardic acid, the principal acidic constituent of CNSL, has received considerable attention as a renewable alternative to petroleum-derived resources. Its application in solvent-free synthesis reduces solvent consumption, lowers chemical waste and supports the principles of green chemistry [3].

The chemistry of Schiff bases has attracted sustained interest owing to the simplicity of their synthesis, their strong affinity for metal ions and the diverse biological properties exhibited by their metal complexes [4,5]. The incorporation of a sulphone moiety into Schiff base frameworks offers additional opportunities to modify their physico-chemical and biological properties [6,7]. Complexation with transition metal ions such as Co(II), Ni(II), Cu(II), and Zn(II) can further influence their coordination geometry, stability and biological performance, making these complexes attractive candidates for medicinal and coordination chemistry [8-10].

In the present study, anacardic acid derived from CNSL was employed as a sustainable acid catalyst under solvent-

free conditions for the synthesis of a sulphone-based Schiff base ligand through the condensation of 4,4′-sulphonyldianiline with furfuraldehyde. The corresponding Co(II), Ni(II), Cu(II), and Zn(II) complexes were characterised using UV-Visible, FT-IR, ^{1}H NMR, ^{13}C NMR, mass spectrometry and SEM techniques. Their antimicrobial activity was evaluated against *Escherichia coli*, *Staphylococcus aureus* and *Candida albicans*, while the Schiff base ligand and its Cu(II) complex were assessed for anticancer activity against the MCF-7 human breast cancer cell line. Molecular docking of the Cu(II) complex with the HER2 receptor was carried out to examine ligand–protein interactions and to complement the experimental biological findings. The combination of a renewable CNSL-derived catalyst, solvent-free synthesis, transition metal complexation, biological evaluation and molecular docking distinguishes the present work from the conventional synthetic approaches and provides a sustainable route for the development of biologically active Schiff base metal complexes.

EXPERIMENTAL

All metal(II) acetate salts employed in this study were obtained from Sigma-Aldrich, USA and used as supplied. The analytical-grade 4,4′-sulfonyldianiline (dapsone) and furfuraldehyde were purchased from TCI Chemicals. HPLC grade solvents were used throughout the synthesis, purification and characterisation of the synthesized compounds.

Extraction of CNSL and catalytic evaluation: Cashew nut shell liquid (CNSL) was extracted from cashew nut shells following the reported procedure [11] and used as a green catalyst for the solvent-free synthesis of the sulphone-based Schiff base ligand. Catalyst optimization identified 0.8 mL of CNSL as the optimum loading, affording an 85% yield within 5 min, while higher catalyst loadings did not improve the reaction results.

Synthesis of Schiff base ligand (L_1): A Schiff base ligand (L_1) was synthesised by reacting 4,4′-sulfonyldianiline (dapsone) (1 mmol) with furfuraldehyde (2 mmol) under solvent free conditions in the presence of 1.2 mL of cashew nut shell liquid (CNSL) as a green catalyst. The reaction mixture was stirred until completion. Subsequently, 4-5 mL of 95% ethanol was added to remove waxy and gelatinous impurities. The catalyst was separated and washed thoroughly with 4-5 mL of petroleum ether, followed by air drying. The crude product was purified by recrystallisation from 95% ethanol to afford the pure Schiff base ligand (L_1) (**Scheme-I**).

Schiff base metal(II) complexes (ML_1a-d): An ethanolic solution of the Schiff base ligand L_1 (1 mmol) was added to an ethanolic solution of the corresponding metal(II) acetate salt (1 mmol) in a 1:1 molar ratio. The reaction mixture was stirred at room temperature for 3 h and then refluxed for an additional 3 h. After completion of the reaction, the resulting metal(II) complex was filtered, washed several times with methanol to remove any unreacted materials and dried under vacuum over anhydrous calcium chloride (**Scheme-I**).

Biological studies

Antimicrobial assay: The antimicrobial activity of the synthesized Schiff base ligand and its metal(II) complexes was evaluated against *Staphylococcus aureus*, *Escherichia coli* and *Candida albicans* using the agar disc diffusion method [12]. Mueller-Hinton agar was employed as the culture medium and chloramphenicol served as the reference drug. Test solutions of the ligand and metal complexes were prepared in DMSO and sterile filter paper discs (6 mm diameter) were impregnated with the respective solutions and dried before use. Fresh microbial suspensions were uniformly spread on Mueller-Hinton agar plates, followed by placement of the impregnated discs onto the inoculated surface. The plates were allowed to dry for 30 min at 37 ºC and subsequently incubated at 36 ºC for 24 h. Antimicrobial activity was assessed by measuring the diameter of the inhibition zone surrounding each disc.

Anticancer assay: The *in vitro* cytotoxic activity of the synthesized Schiff base ligand and its Cu(II) complex was investigated against the MCF-7 human breast cancer cell line using the MTT assay following the reported procedure [13] with minor modifications. Cells were seeded in 24-well plates at a density of 1×10^5 cells per well and maintained at 37 ºC in a humidified atmosphere containing 5% CO_2. Once the cell monolayer reached approximately 80-90% confluence, different concentrations of the test compounds were added and the cells were incubated for 24 h.

Following treatment, the culture medium was discarded and the cells were gently rinsed with phosphate-buffered saline (PBS, pH 7.4). A 100 µL aliquot of MTT solution (0.5%, 5 mg mL^{-1}) was then added to each well and the plates were incubated for 4 h to allow intracellular formation of formazan crystals. After removing the supernatant, 1 mL of DMSO was added to dissolve the crystals. Absorbance was recorded at 570 nm using a UV-Visible spectrophotometer, with DMSO as blank. Cell viability was calculated from the measured absorbance values and IC_{50} values were obtained from dose-response curves. Untreated cells served as the control, each experiment was performed in triplicate and the results were expressed as the mean of three independent measurements [14].

$$\text{Cell viability (\%)} = \frac{A_{570} \text{ of treated cells}}{A_{570} \text{ of control cells}} \times 100$$

Molecular docking: The molecular structures of the Schiff base ligand (L_1) and its Cu(II) complex (CuL_1) were constructed using ChemAxon's Marvin 17.21.0 and geometry optimised with Avogadro 1.2.0 [15]. Molecular docking was carried out to examine the binding of CuL_1 with the human epidermal growth factor receptor 2 (HER2), a therapeutic target associated with breast cancer. The crystal structure of HER2 (PDB ID: 3MZW) was obtained from the Protein Data Bank (PDB) [16]. Prior to docking, crystallographic water molecules were removed and polar hydrogen atoms were added to the protein structure. AD4 atom types were assigned and ligand rotatable bonds were defined using AutoDock Tools 1.5.6.

The docking grid was centered on the HER2 binding pocket comprising residues P398, W430, E379, R477, R434, D399, Q376, L397, Q404, S396, T504 and E485 [17]. The docking calculations were performed using a grid spacing of 0.67 Å with a grid box size of 50 × 50 × 50 points [18]. AutoDock 4.0.1 was employed to predict the binding conformations and estimate the binding energies of the ligand and CuL_1

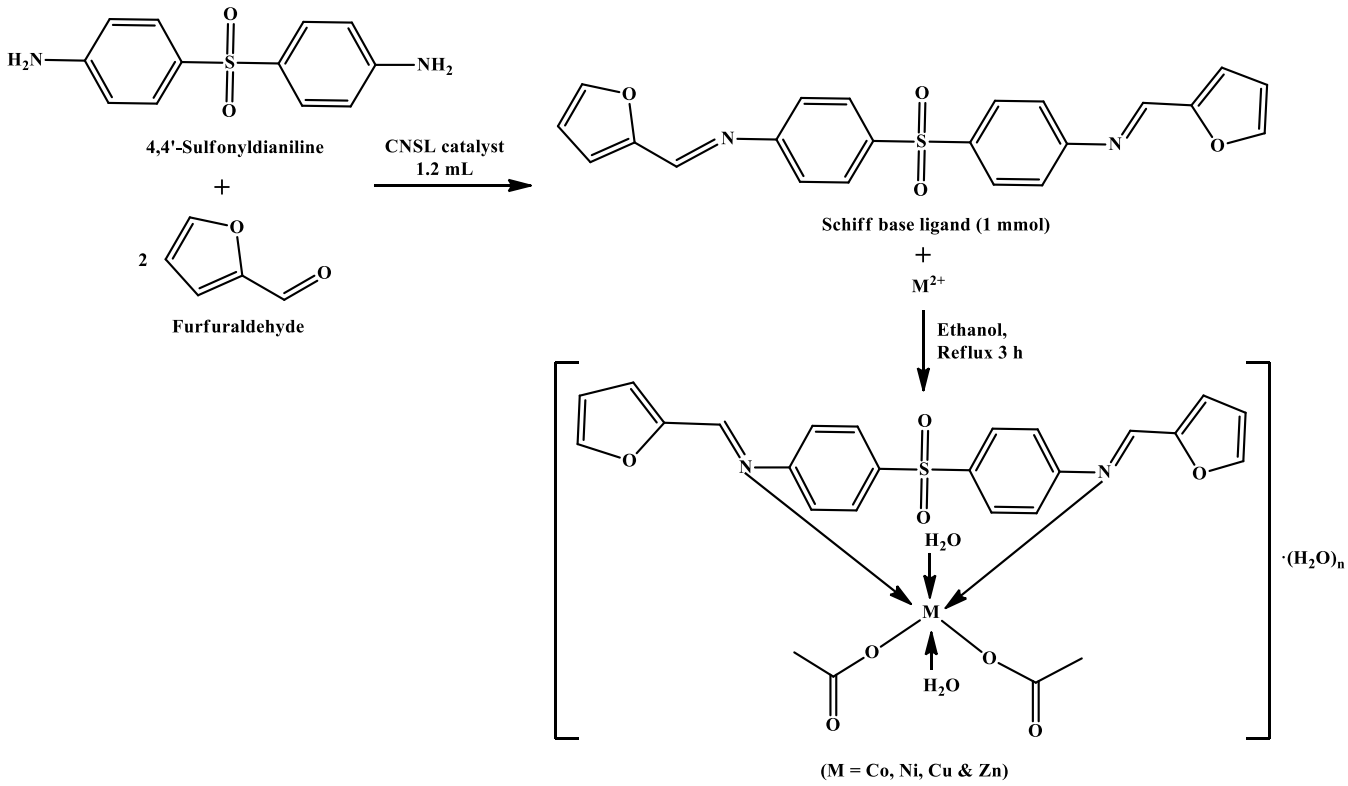

Scheme-I: Synthesis of the Schiff base ligand (L_1) from 4,4′-sulfonyldianiline and furfuraldehyde and metal(II) complexes (**ML_1a-d**)

complex. Ligand–protein interactions were analysed using AutoDock Tools, while three-dimensional representations of the docked complexes were generated with UCSF Chimera [19].

RESULTS AND DISCUSSION

The Schiff base ligand (L_1) was synthesised by condensing 4,4′-sulfonyldianiline (dapsone, 1 mmol) with furfuraldehyde (2 mmol) under solvent-free conditions using cashew nut shell liquid (CNSL) as a green catalyst (**Scheme-I**). Under the optimized reaction conditions, the desired ligand was isolated in an 85% yield. The catalytic efficiency of CNSL arises from the anacardic acid present in the extract, which promotes the condensation reaction leading to the formation of the azomethine (–CH=N–) linkage. The elemental analysis of the Schiff base ligand (L_1) and its metal(II) complexes (**ML_1a-d**) agreed well with the proposed molecular compositions (Table-1). Solubility studies revealed that the ligand and its metal(II) complexes were sparingly soluble in methanol, ethanol, acetone and chloroform, whereas complete dissolution was achieved in DMSO and DMF solvents. Molar conductance measurements were carried out in DMSO and the obtained values (Table-1) showed that the metal(II) complexes behave as ionic species in solution [20].

The proposed mechanism (**Scheme-II**) involves the nucleophilic attack of the amino group of 4,4′-sulphonyldianiline on the carbonyl carbon of furfuraldehyde to form a carbinolamine intermediate. Proton transfer followed by the loss of water gives the azomethine (–CH=N–) linkage. The reaction proceeds at both amino groups of dapsone to afford the *bis*-Schiff base ligand. The CNSL catalyst participates in the proton-transfer steps and is regenerated during the course of the reaction under solvent-free conditions.

FT-IR spectral studies: In the FT-IR spectra (Fig. 1) shows that green synthesised Schiff based ligand L_1 functions as a bidentate ligand by coordinating through the azomethine nitrogen atom and an oxygen atom of the acetate group, while coordinated water molecules are present in the metal complexes [21]. The free ligand exhibits a prominent azomethine ν(C=N) band at 1632 cm^{-1}. Following the complex formation, this absorption shifts to the 1623-1590 cm^{-1} region, further confirmed the coordination of the azomethine nitrogen to the metal center [22].

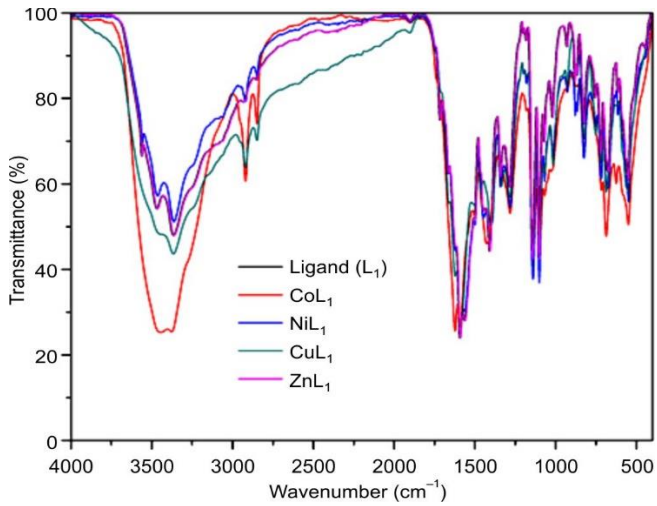

Fig. 1. FT-IR spectra of the Schiff base ligand (L_1) and its metal(II) complexes (**ML_1a-d**)

TABLE-1
ELEMENTAL ANALYSIS AND PHYSICO-CHEMICAL PROPERTIES OF
THE SCHIFF BASE LIGAND (L_1) AND ITS METAL(II) COMPLEXES (**ML_1a-d**)

Compound	m.f.	m.w.	Colour	m.p. (°C)	Molar conductance (Ω^{-1} cm^2 mol^{-1})	Elemental analysis (%): calcd. (found)			
						C	H	N	Metal
Ligand (L_1)	$C_{22}H_{16}N_2O_4S$	404	Brown	120	–	64.55 (65.34)	3.00 (3.99)	6.05 (6.93)	–
ML_1a	$C_{26}H_{28}N_2O_{11}SCo$	635	Reddish brown	220	18.16	55.12 (53.14)	5.45 (5.04)	7.23 (7.41)	7.81 (7.27)
ML_1b	$C_{26}H_{28}N_2O_{11}SNi$	636	Brown	223	15.13	55.10 (54.12)	5.32 (5.43)	7.23 (7.32)	7.70 (7.65)
ML_1c	$C_{26}H_{24}N_2O_9SCu$	603	Dark brown	245	20.21	53.42 (53.70)	5.24 (5.00)	7.96 (7.64)	8.90 (9.52)
ML_1d	$C_{26}H_{26}N_2O_{12}SZn$	622	Yellow	232	32.65	55.48 (54.05)	5.42 (5.20)	7.76 (7.49)	8.87 (9.48)

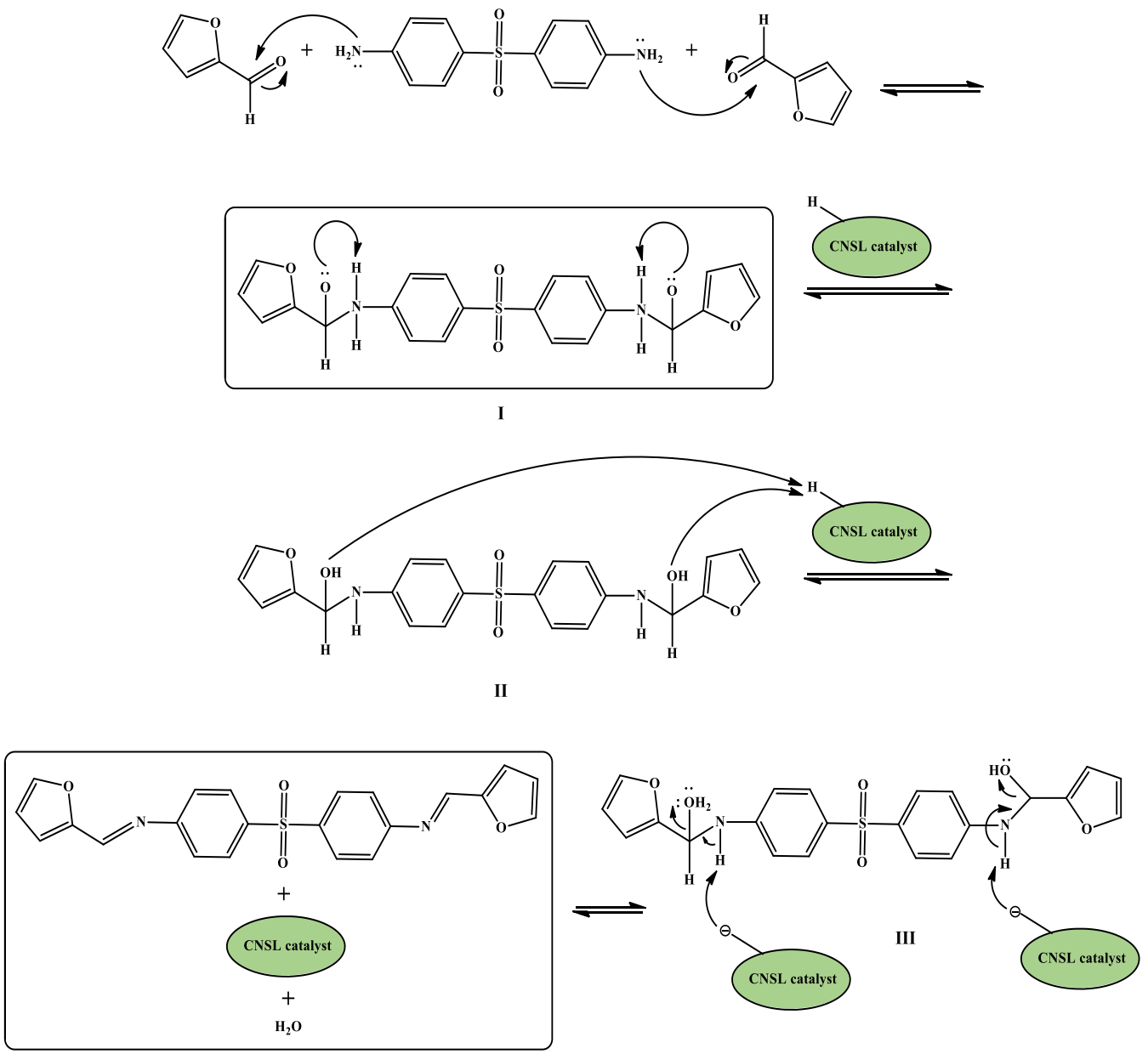

Scheme-II: Proposed mechanism for the formation of the Schiff base ligand in the presence of CNSL catalyst

The spectra of the metal(II) complexes exhibit additional bands at 1735-1715 cm^{-1} and 1573-1560 cm^{-1}, which is assigned to the asymmetric ν_{asym}(OAc) and symmetric ν_{asym}(OAc) stretching vibrations of coordinated acetate groups, respectively [23]. Broad absorptions between 3467 and 3378 cm^{-1}, together with bands in the 876-860 cm^{-1} region, are the characteristic of coordinated water molecules [24]. The Schiff base ligand and its metal(II) complexes also exhibit SO_2 stretching bands at 1344-1340 cm^{-1}. Their positions remain essentially unchanged after metal coordination, which implies that the sulphone oxygen atoms are not involved in bonding with the metal ions [25]. New absorptions appearing in the low-frequency region (555-516 cm^{-1}) are attributed to ν(M–N) vibrations, providing further evidence for coordination through the azomethine nitrogen atom [26].

NMR spectral studies: The ^1H and ^{13}C NMR spectra of the Schiff base ligand (L_1) confirmed the successful formation of the azomethine (–CH=N–) moiety. The spectra were recorded in DMSO-d_6 using TMS as the internal reference and are shown in Fig. 2a-b. In the ^1H NMR spectrum, a multiplet appearing in the region of δ 6.05-7.96 ppm was assigned to the aromatic protons. A characteristic singlet observed at δ 9.82 ppm corresponds to the azomethine proton (–CH=N–), confirming the condensation of the aldehyde and amine to form the Schiff base ligand. The ^{13}C NMR spectrum displayed a distinct resonance at δ 154.89 ppm, which was attributed to the azomethine carbon (C=N), further supporting the successful formation of the ligand. These spectral characteristics are in good agreement with those reported for structurally related Schiff base compounds in the literature [27].

Electronic spectral and magnetic moment studies: The electronic absorption spectra of the Schiff base ligand (L_1) and its metal(II) complexes (**ML_1a-d**) were recorded in DMSO. The free Schiff base ligand exhibited two characteristic absorption bands at 255 and 360 nm, which are assigned to the $\pi \rightarrow \pi^*$ transition of the aromatic benzene ring and the $n \rightarrow \pi^*$ transition of the azomethine (C=N) group, respectively. Upon complexation, these absorption bands shifted towards lower wavelengths (hypsochromic shift), which can be attributed to the coordination of the azomethine nitrogen atom with the metal ions [28].

The electronic spectrum of the Co(II) complex, (**ML_1a**), exhibited absorption bands at 405 and 620 nm, assigned to the $^4T_1g(F) \rightarrow {}^4T_1g(P)$ and $^4T_1g(F) \rightarrow {}^4A_2g(F)$ transitions, respectively. Its magnetic moment of 4.25 B.M. is characteristic of an octahedral environment around the Co(II) ion [29]. The Ni(II) complex, (**ML_1b**), displayed absorption bands at 470 and 560 nm, corresponding to the $^3A_2g(F) \rightarrow {}^3T_1g(P)$ and $^3A_2g(F) \rightarrow {}^3T_1g(F)$ transitions, respectively. A magnetic moment of 2.95 B.M. agrees well with an octahedral arrangement of the Ni(II) ion [30]. The Cu(II) complex, (**ML_1c**), exhibited a broad absorption band at 585 nm arising from the $^2B_{1g} \rightarrow {}^2A_{1g}$ transitions. The measured magnetic moment of 1.47 B.M. is in agreement with a square-planar geometry around the Cu(II) centre [31]. The Zn(II) complex, (**ML_1d**), exhibited a medium intensity absorption band at 456 nm, assigned to a ligand-to-metal charge transfer (LMCT) transition. Its diamagnetic behaviour is characteristic of a d^{10} electronic configuration and is compatible with an octahedral coordination environment around the Zn(II) ion [32].

Mass spectral studies: The ESI-mass spectrum of the Schiff base ligand (L1) exhibited a molecular ion peak at *m/z* 406 [M+2], consistent with its monomeric molecular formula, $C_{22}H_{16}N_2O_4S$. The mass spectra of the metal complexes displayed molecular ion peaks at *m/z* 635.18 [M+1], 636.54 $[M]^+$, 601.12 [M+2] and 622.13 [M+1], corresponding to the molecular formulae $C_{26}H_{28}N_2O_{11}SCo$ (**ML_1a**), $C_{26}H_{28}N_2O_{11}SNi$ (**ML_1b**), $C_{26}H_{24}N_2O_9SCu$ (**ML_1c**) and $C_{26}H_{26}N_2O_{12}SZn$ (**ML_1d**), respectively [33]. The observed molecular ion peaks are in good agreement with the proposed stoichiometry of the complexes. Elemental analysis data are likewise consistent with the calculated compositions, providing additional evidence for the assigned molecular formulations.

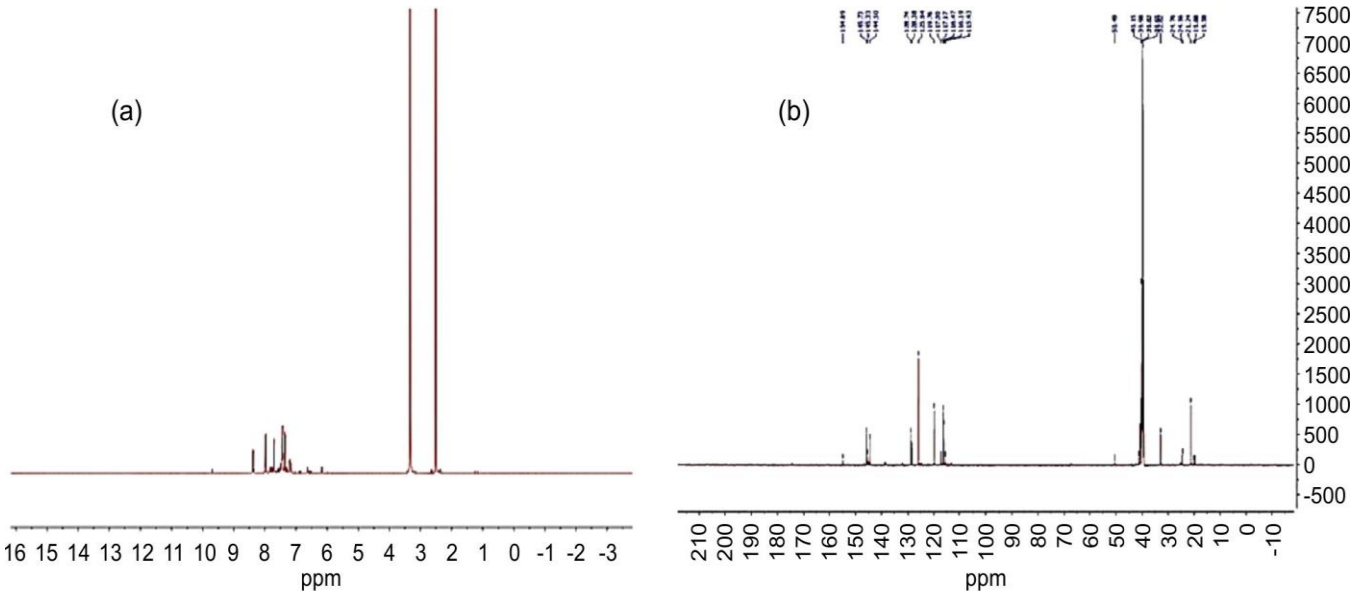

Fig. 2. ^1H NMR (a) and ^{13}C NMR (b) spectra of the ligand (L_1)

SEM studies: SEM analysis was carried out to examine the surface morphology of the Schiff base ligand and its metal complexes, and the corresponding micrographs are shown in Fig. 3. Coordination of the metal ions to the donor sites of the ligand results in distinct changes in surface morphology, as evident from the SEM images [34]. The Schiff base ligand exhibits a randomly distributed cracked needle-like structure. The Co(II) and Ni(II) complexes are composed of small, irregularly shaped grains. The Zn(II) complex possesses a nanocrystalline morphology with a crushed rock-like texture, whereas the Cu(II) complex exhibits a microcrystalline morphology resembling a coral reef-like texture. These morphological differences are consistent with the formation of metal complexes and reflect the influence of the coordinated metal ions on the surface characteristics of the ligand.

Antimicrobial activity: The *in vitro* antimicrobial activity of the Schiff base ligand (L_1) and its mononuclear metal(II) complexes (**ML_1a-d**) was evaluated by the disk diffusion method against the Gram-positive bacterium *S. aureus*, the Gram-negative bacterium *E. coli* and the fungal strain *C. albicans*. Tetracycline and fluconazole were used as the reference antibacterial and antifungal drugs, respectively, whereas DMSO was employed as the negative control. The metal(II) complexes displayed greater antimicrobial activity than the free Schiff base ligand against all the tested microorganisms, reflecting the favourable influence of metal coordination on the biological properties of the ligand [35].

Among the synthesised complexes, the Cu(II) complex (**ML_1c**) exhibited the highest antibacterial and antifungal activity, whereas the Co(II), Ni(II) and Zn(II) complexes showed comparatively lower inhibitory effects (Table-2). The superior activity of the Cu(II) complex can be explained by the combined influence of the Cu(II) ion and the chelation effect. According to Tweedy's chelation theory, coordination of the ligand with the Cu(II) ion reduces the polarity of the metal centre through partial sharing of its positive charge with the donor atoms and electron delocalisation within the chelate ring. The resulting increase in lipophilicity enhances the ability of the complex to penetrate the lipid membrane of microbial cells. The increased lipophilicity of the Cu(II) complex facilitates its passage through the microbial cell membrane, where it interferes with essential cellular functions, including protein synthesis, leading to inhibition of microbial growth and proliferation [36].

TABLE-2
ZONE OF INHIBITION (mm) OF THE SCHIFF BASE LIGAND (L_1) AND ITS METAL(II) COMPLEXES AGAINST SELECTED MICROORGANISMS

Sample	Zone of inhibition (mm)		
	Gram-positive	Gram-negative	Fungi
	S. aureus	*E. coli*	*C. albicans*
Ligand (L_1)	29	11	12
ML_1a	35	11	20
ML_1b	34	16	20
ML_1c	38	18	22
ML_1d	33	12	20
Standard	31	8	9

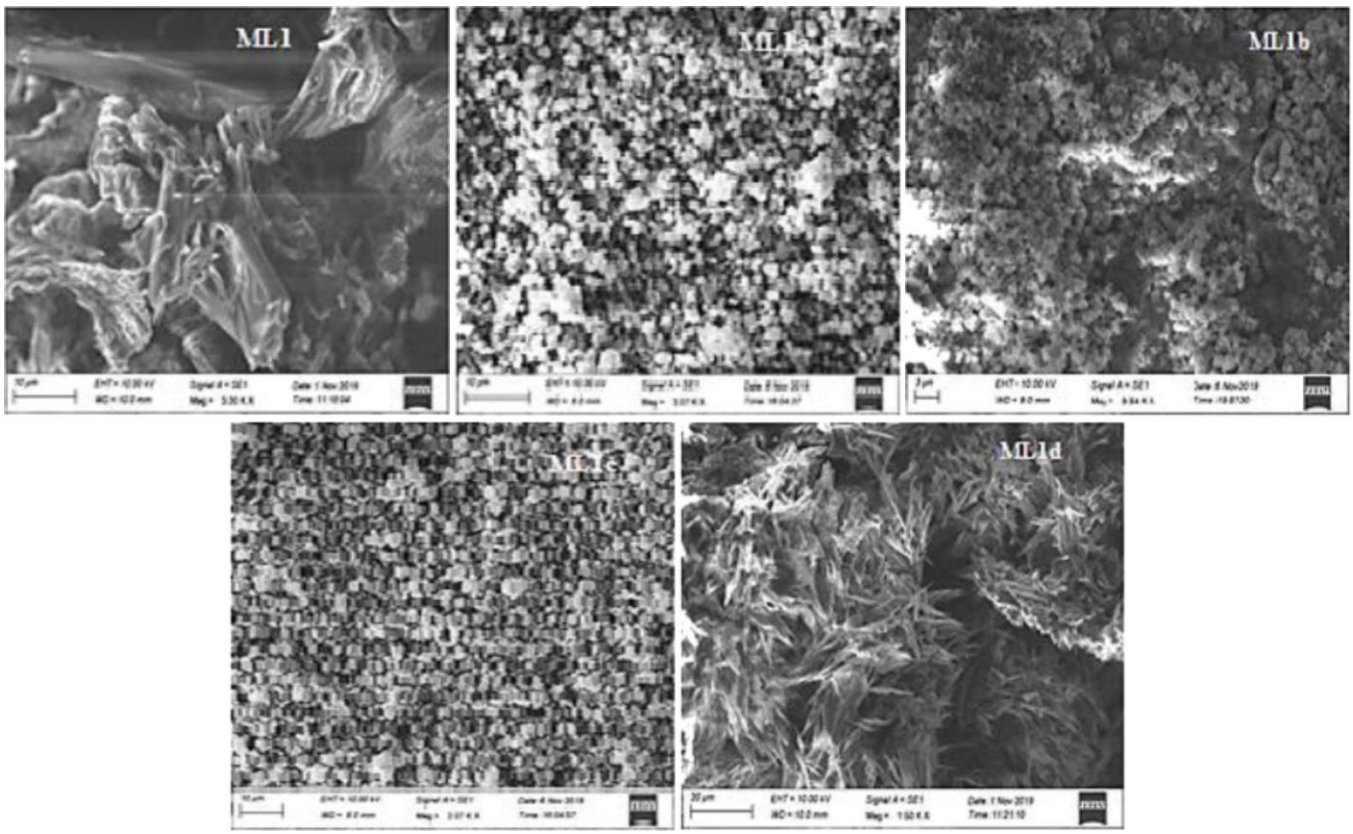

Fig. 3. SEM Micrographs of the Schiff base ligand (L_1) and its metal(II) complexes (**ML_1a-d**)

***In vitro* anticancer activity:** The anticancer activity of the Schiff base ligand (**L_1**) and its Cu(II) complex (**ML_1c**) was evaluated against the human breast cancer cell line MCF-7 using the MTT assay (Fig. 4). Absorbance was measured at 560 nm after treatment with different concentrations (20-100 µg/mL) of the test compounds, and the results are shown in Table-3. The Cu(II) complex (**ML_1c**) exhibited higher cytotoxic activity than the free ligand, with an IC_{50} value of 52.80 µg/mL, while **L_1** exhibited an IC_{50} value of 60.20 µg/mL. The lower IC_{50} value of the Cu(II) complex suggests that coordination with the metal ion enhances the antiproliferative properties of the ligand. Although the Cu(II) complex was more active than the free ligand, its cytotoxic effect remains moderate when compared with clinically established anticancer agents such as cisplatin and doxorubicin. The present results identify the Cu(II) complex as a suitable candidate for further structural modification and biological evaluation.

TABLE-3
In vitro ANTICANCER ACTIVITY OF THE SCHIFF BASE LIGAND (L_1) AND Cu(II) COMPLEX (ML_1c) AGAINST MCF-7 CELLS

Conc. (µg/mL)	Cell viability (%)		IC_{50} (µg/mL)	
	L_1	ML_1c	L_1	ML_1c
20	30.07	35.33		
40	46.61	45.86		
60	51.12	54.13	60.20	52.80
80	58.61	60.90		
100	63.15	68.42		

Molecular docking: HER2 is overexpressed in several human malignancies, particularly aggressive breast cancers, making it an attractive target for diagnosis and targeted therapy. The 58-amino-acid affibody molecule ZHER2 was engineered to bind HER2 with high affinity. Unlike therapeutic antibodies such as pertuzumab [37] and trastuzumab [38], ZHER2 recognizes a distinct conformational epitope on the HER2 receptor. Small-molecule HER2 inhibitors continue to attract attention because of their potential advantages in bioavailability, tissue penetration, and ease of synthesis [39,40]. Schiff base metal complexes have also been reported to exhibit promising anticancer properties against different cancer cell lines [41]. In the present study, molecular docking was performed to investigate the binding of the Schiff base ligand (L_1) and its Cu(II) complex with the HER2 receptor (PDB ID: 3MZW). Chain A of the HER2 crystal structure (2.90 Å resolution) was used for docking. The predicted binding conformations are shown in Fig. 5, while the calculated binding energies, inhibition constants, intermolecular energies, hydrogen bonds and hydrophobic interactions are shown in Table-4.

Docking of the free ligand (L_1) with HER2 generated two hydrogen bonds and seven hydrophobic interactions involving residues W430, E485, G486, L487, A488, C489, H490, Q491, P501 and G502. The ligand occupied an interface area of 107.6 $Å^2$ within Domain III of the HER2 receptor and exhibited a calculated binding energy of -2.93 kcal/mol with an inhibition constant (Ki) of 7.07 mM. The NH group of H490 formed a weak hydrogen bond with the ligand oxygen atom at 3.08 Å, whereas the oxygen atom of E485 formed a stronger hydrogen bond with the ligand NH group at a distance of 2.09 Å [42]. Further stabilization arised from several π-related interactions. The five-membered ring centroid (Cg1) of H490 participated in an anion···π interaction with the ligand oxygen atom at 3.3 Å. The benzene ring centroid (Cg2) of the ligand formed an anion···π interaction with the oxygen atom of A488 at 4.3 Å and a weak N–H···π interaction with G486 at 5.3 Å. Another aromatic ring centroid (Cg3) established anion···π interactions with the oxygen atoms of L487 and E485 at distances of 4.2 and 4.1 Å, respectively. The fourth aromatic ring centroid (Cg4) formed a C–H···π interaction with L487 and a T-shaped π–π interaction with W430 at 4.5 and 4.1 Å, respectively. These non-covalent interactions contributed to an intermolecular energy of -5.32 kcal/mol.

The CuL_1 complex formed seven hydrogen bonds and one hydrophobic interaction with residues D399, Q404, W430, R434, P501, P503, T504, and Q505. The calculated binding energy was -2.86 kcal/mol with a Ki value of 8.00 mM. The NE2 atom of Q505 formed a hydrogen bond with the O4 atom of CuL_1 at 3.22 Å. The OG1 atom of T504 interacted with the O6, O3 and N2 atoms of CuL_1 through hydrogen

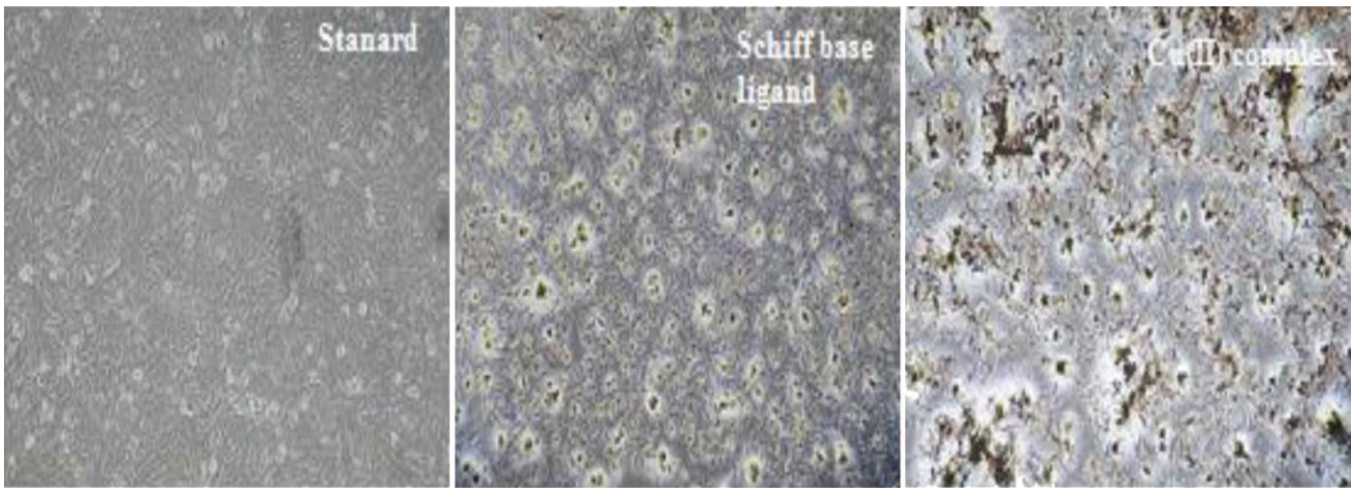

Fig. 4. Cytotoxic activity of the standard drug, Schiff base ligand (L_1) and Cu(II) complex (**ML_1c**) against MCF-7 cells

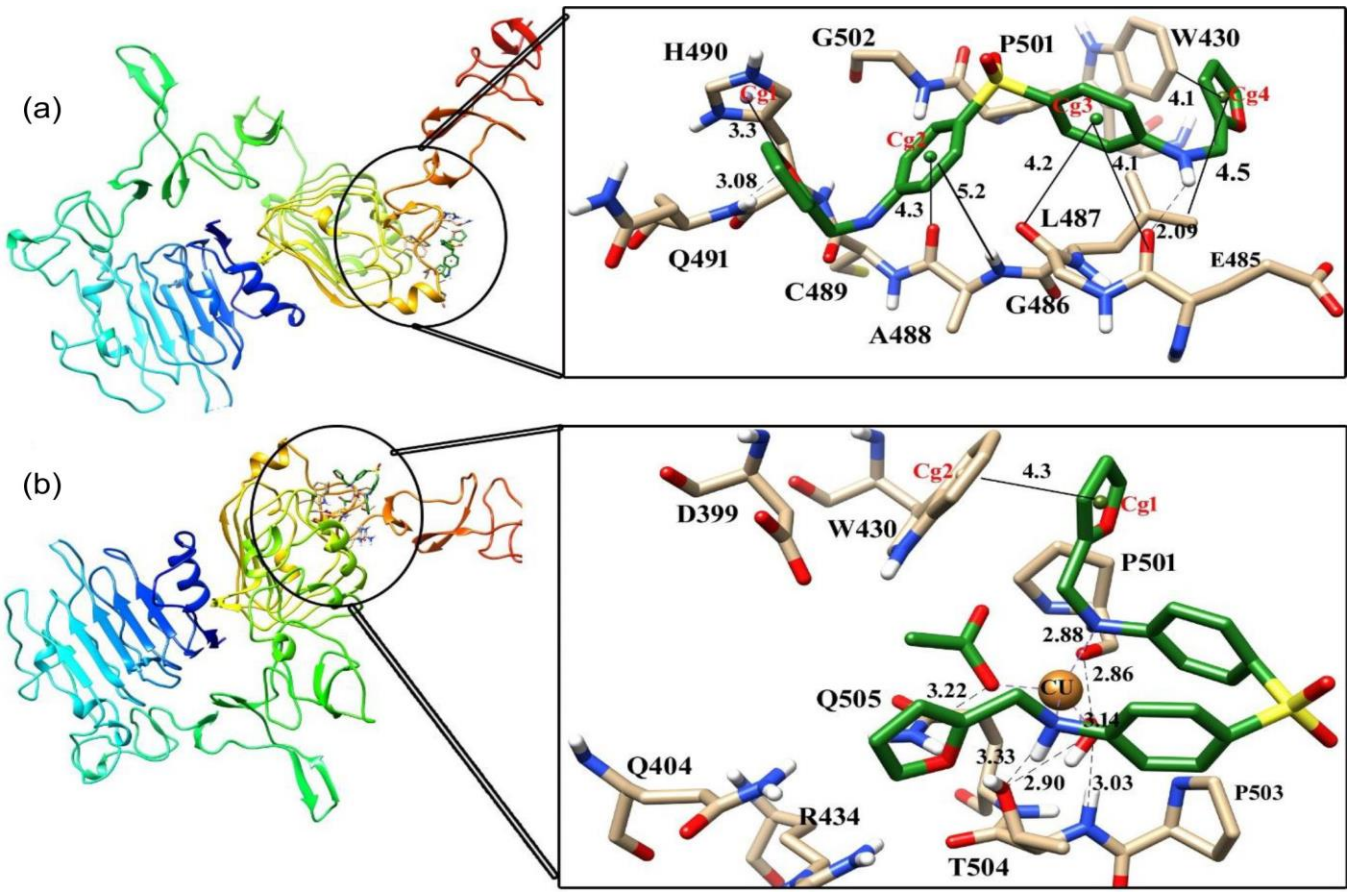

Fig. 5. The molecular interaction of ligand (L_1) and CuL_1 with domain III of HER2 protein and the zoomed image shows the polar and non-polar residues actively contributing for the interaction. (a) Ligand interaction with HER2 protein, (b) CuL_1 interaction with HER2 protein. Here, the hydrogen bonds are shown in black dotted lines where the special types of hydrophobic interactions were shown in back line. The coordination interactions were shown in blue dotted lines and the centroid of the rings were mentioned as Cg

TABLE-4
MOLECULAR INTERACTION OF LIGAND (L_1) AND $CuL1_1$ (**ML_1c**) WITH HER2 PROTEIN

Ligand and copper(II) complex	Binding energy (kcal/mol)	Inhibition constant (K_i) (mM)	Intermolcular energy (kcal/mol)	Interacting residues	Bonding distance		
					Ligand (atom)	Protein (atom)	Distance (Å)
Ligand (L_1)	-2.93	7.07	-5.32	W430, E485, G486, L487, A488, C489, H490, Q491,G502, P501	Hydrogen bonding interactions		
					L-O	H490-NH	3.08
					L-NH	E485-O	2.09
					Special type of interactions		
				Anion···π	L-O	Cg1-H490	3.3
				Anion···π	Cg2-L	O-A488	4.3
				N-H···π	Cg2-L	NH-G486	5.2
				Anion···π	Cg3-L	O-L487	4.2
				Anion···π	Cg3-L	O-E485	4.1
				C-H···π	Cg4-L	CH-L487	4.5
				T-Shaped···π	Cg4-L	CZ-W430	4.1
CuL_1 (**ML_1c**)	-2.86	8.00	-6.14	D399, Q404, W430, R434, P501, P503, T504, Q505	Hydrogen bonding interactions		
					CuL1-O4	Q505-NE2	3.22
					CuL1-O6	T504-OG1	3.14
					CuL1-O3	T504-OG1	2.90
					CuL1-N2	T504-OG1	3.33
					CuL1-O3	T504-N	3.03
					CuL1-O3	P501-O	2.86
					CuL1-N1	P501-O	2.88
					Special type of interactions		
				π···π stacking	CuL_1-Cg1	W430-Cg2	4.3

bonds measuring 3.14, 2.90, and 3.33 Å, respectively, one of which was water-mediated. The backbone nitrogen atom of T504 formed another water-mediated hydrogen bond with the O3 atom of CuL_1 at 3.03 Å. Two additional hydrogen bonds were observed between the oxygen atom of P501 and the O3 and N1 atoms of CuL_1 at distances of 2.86 and 2.88 Å, respectively. A π-related hydrophobic interaction was identified between the aromatic centroid of CuL_1 and the indole ring centroid of W430 at a distance of 4.3 Å.

Comparison of the docking results shows that the free ligand and the Cu(II) complex possess comparable binding affinities toward the HER2 receptor. The difference in the calculated binding energy is small (-2.93 and -2.86 kcal/mol), whereas the Cu(II) complex forms a larger number of hydrogen bonds. Both compounds interact with the HER2 binding region through a combination of hydrogen-bonding and hydrophobic contacts. Since docking scores alone cannot accurately predict binding affinity, these calculations should be regarded as supportive computational evidence rather than conclusive proof of stronger HER2 binding. The Cu(II) complex was selected as the most promising compound since it exhibited superior *in vitro* cytotoxic activity against MCF-7 cells together with a favourable docking profile. Experimental HER2 inhibition assays, molecular dynamics simulations and binding free-energy calculations are required to validate the proposed binding mode and clarify its mechanism of action [11].

Conclusion

This work highlights the synthesis and biological evaluation of a new Schiff base ligand prepared from furfuraldehyde and 4,4′-sulfonyldianiline (dapsone) using a solvent-free, CNSL-catalysed green synthetic approach under ambient conditions. Mononuclear Co(II), Ni(II), Cu(II) and Zn(II) complexes were synthesised in a 1:1 metal-to-ligand ratio and characterised by elemental analysis and spectroscopic techniques. The physico-chemical studies assigned octahedral geometries to the Co(II), Ni(II) and Zn(II) complexes, while the Cu(II) complex adopted a square-planar geometry. SEM analysis revealed distinct morphological changes following metal coordination. Biological evaluation showed that all metal(II) complexes exhibited higher antimicrobial activity than the free ligand against the studied bacteria, with the Cu(II) complex displaying the highest activity. MTT assay against MCF-7 cells revealed moderate cytotoxicity, with the Cu(II) complex exhibiting a lower IC_{50} value than the free ligand. Molecular docking demonstrated that both the Schiff base ligand and the Cu(II) complex interact favourably with the HER2 receptor through multiple hydrogen-bonding and hydrophobic interactions. The calculated docking scores were comparable and do not, by themselves, establish the Cu(II) complex as a stronger HER2 binder. Considering its superior *in vitro* cytotoxic activity together with its favourable interaction profile, the Cu(II) complex emerges as the most promising candidate.

CONFLICT OF INTEREST

The authors declare that there is no conflict of interests regarding the publication of this article.

DECLARATION OF AI-ASSISTED TECHNOLOGIES

During the preparation of this manuscript, the authors used an AI-assisted tool(s) to improve the language and no data, results or scientific conclusions were generated by AI. All analyses, interpretations and conclusions are the authors' own. The authors reviewed and edited the content and take full responsibility for the published work.

REFERENCES

1. A.M. Hassan, A.O. Said, B.H. Heakal, A. Younis, W.M. Aboulthana and M.F. Mady, *ACS Omega*, **7**, 32418 (2022); https://doi.org/10.1021/acsomega.2c03911
2. S. Boinapalli, A. Anil Kumar and Ch. Abraham Lincoln, *Int. J. Adv. Chem.*, **13**, 5948 (2017); https://doi.org/10.24297/jac.v13i12.6124
3. M.N. Esfahani, *Crystallogr. Rep.*, **54**, 1135 (2009); https://doi.org/10.1134/S1063774509070049
4. C. Boulechfar, H. Ferkous, A. Delimi, A. Djedouani, A. Kahlouche, A. Boublia, A.S. Darwish, T. Lemaoui, R. Verma and Y. Benguerba, *Inorg. Chem. Commun.*, **150**, 110451 (2023); https://doi.org/10.1016/j.inoche.2023.110451
5. G. Behera, R. Sidhanty, A.K. Sutar and T. Maharana, *Discov. Chem.*, **3**, 119 (2026); https://doi.org/10.1007/s44371-026-00536-5
6. K.D. Gaikwad, R.M. Khobragade, S.A. Deodware, P.A. Ubale, P.C. Dhale, R.M. Ovhal, C. Shivamallu, V.M. Ankegowda, H.L. Raghavendra, S.H. Gaikwad and S.P. Kollur, *Results Chem.*, 4, 100617 (2022); https://doi.org/10.1016/j.rechem.2022.100617
7. M.M. Sayed, M. Abdel-Hakim, M.H. Mahross and K.I. Aly, *Sci. Rep.*, **12**, 12878 (2022); https://doi.org/10.1038/s41598-022-17042-0
8. A. Yadav, S. Yadav, A. Kamboj, B. Phogat and K. Poonia, *Inorg. Chem. Commun.*, **181**, 115151 (2025); https://doi.org/10.1016/j.inoche.2025.115151
9. I.P. Ejidike and P.A. Ajibade, *Rev. Inorg. Chem.*, **35**, 191 (2015); https://doi.org/10.1515/revic-2015-0007
10. R. Malav and S. Ray, *RSC Adv.*, **15**, 22889 (2025); https://doi.org/10.1039/D5RA03626G
11. C.K. Moorthy, T. Gomathi, M. Kannan and T.M. Priya, *Results Chem.*, **14**, 102131 (2025); https://doi.org/10.1016/j.rechem.2025.102131
12. R. Zaky, A. Fekri, Y.G. Abou El-Reash, H.M. Youssef and A.Y. Kareem, *Egypt. J. Basic Appl. Sci.*, **3**, 272 (2016); https://doi.org/10.1016/j.ejbas.2016.06.004
13. T. Mosmann, *J. Immunol. Methods*, **65**, 55 (1983); https://doi.org/10.1016/0022-1759(83)90303-4
14. I. Waziri, S. Sookai, T.L. Yusuf, K.A. Olofinsan and A.J. Muller, *Appl. Organomet. Chem.*, **39**, e70162 (2025); https://doi.org/10.1002/aoc.70162
15. M.D. Hanwell, D.E. Curtis, D.C. Lonie, T. Vandermeersch, E. Zurek and G.R. Hutchison, *J. Cheminform.*, **4**, 17 (2012); https://doi.org/10.1186/1758-2946-4-17
16. C. Eigenbrot, M. Ultsch, A. Dubnovitsky, L. Abrahmsén and T. Härd, *Proc. Natl. Acad. Sci. USA*, **107**, 15039 (2010); https://doi.org/10.1073/pnas.1005025107
17. G.M. Morris, D.S. Goodsell, R.S. Halliday, R. Huey, W.E. Hart, R.K. Belew and A.J. Olson, *J. Comput. Chem.*, **19**, 1639 (1998); https://doi.org/10.1002/(SICI)1096-987X(19981115)19:14<1639::AID-JCC10>3.0.CO;2-B
18. E.F. Pettersen, T.D. Goddard, C.C. Huang, G.S. Couch, D.M. Greenblatt, E.C. Meng and T.E. Ferrin, *J. Comput. Chem.*, **25**, 1605 (2004); https://doi.org/10.1002/jcc.20084
19. M. Kannan, P. Manivel, K. Geetha, J. Muthukumaran, H.S.P. Rao and R. Krishna, *J. Chem. Biol.*, **5**, 151 (2012); https://doi.org/10.1007/s12154-012-0084-z
20. K. Muthu, M. Panneerselvam, M. Jayaraman, N.S. Topno, A.A. Das and K. Ramadas, *J. Mol. Model.*, **18**, 4865 (2012); https://doi.org/10.1007/s00894-012-1489-x

21. B. Parasuraman, J. Rajendran and R. Rangappan, *Orient. J. Chem*., **33**, 1223 (2017); https://doi.org/10.13005/ojc/330321
22. K. Andiappan, A. Sanmugam, E. Deivanayagam, K. Karuppasamy, H.-S. Kim and D. Vikraman, *Sci. Rep*., **8**, 3054 (2018); https://doi.org/10.1038/s41598-018-21366-1
23. J.K. Sebastian, M.K. Muraleedharan Nair and S. Sasi, *Rasayan J. Chem.*, **15**, 1202 (2022); https://doi.org/10.31788/RJC.2022.1526789
24. W. Al Zoubi, A.A.S. Al-Hamdani and M. Kaseem, *Appl. Organomet. Chem.*, **30**, 810 (2016); https://doi.org/10.1002/aoc.3506
25. A.S. Abu-Khadra, R.S. Farag and A.E.-D.M. Abdel-Hady, *Am. J. Anal. Chem.*, **7**, 233 (2016); https://doi.org/10.4236/ajac.2016.73020
26. M.S. Nair, D. Arish and R.S. Joseyphus, *J. Saudi Chem. Soc*., **16**, 83 (2012); https://doi.org/10.1016/j.jscs.2010.11.002
27. A.T. Bader, B.I. Al-Abdaly and I. Jassim, *J. Pharm. Sci. Res*., **11**, 2062 (2019).
28. D. Gangrade and S. Lad, *J. Chem. Pharm. Res*., **8**, 1132 (2016).
29. S.H. Kathim, Wasit J. Pure Sci., **4**, 254 (2023); https://doi.org/10.31185/wjps.263
30. J. Devi, N. Batra and R. Malhotra, *Spectrochim. Acta A Mol. Biomol. Spectrosc.*, **97**, 397 (2012); https://doi.org/10.1016/j.saa.2012.06.026
31. S.A. Khan and M. Murtuza, *Int. J. Curr. Res. Chem. Pharm. Sci*., **10**, 1 (2023).
32. T. Vijayan, M. Pugazhenthi, A. Nasirian, J. Kim, G. Kasi, and A. Jayamani, *Bull. Korean Chem. Soc*., **43**, 1284 (2022); https://doi.org/10.1002/bkcs.12618
33. M. Enamullah, M.A. Islam and C. Janiak, *J. Mol. Struct*., **1122**, 331 (2016); https://doi.org/10.1016/j.molstruc.2016.05.093
34. M. Usharani, E. Akila and R. Rajavel, *Int. J. Adv. Sci. Res*., **2**, 274 (2013).
35. N.K. Chaudhary and P. Mishra, *Bioinorg. Chem. Appl*., **2017**, 6927675 (2017); https://doi.org/10.1155/2017/6927675
36. A.R. Patil, K.J. Donde, S.S. Raut, V.R. Patil and R.S. Lokhande, *J. Chem. Pharm. Res*., **4**, 1413 (2012).
37. H.-S. Cho, K. Mason, K.X. Ramyar, A.M. Stanley, S.B. Gabelli, D.W. Denney and D.J. Leahy, *Nature*, **421**, 756 (2003); https://doi.org/10.1038/nature01392
38. M.C. Franklin, K.D. Carey, F.F. Vajdos, D.J. Leahy, A.M. de Vos and M.X. Sliwkowski, *Cancer Cell*, **5**, 317 (2004); https://doi.org/10.1016/S1535-6108(04)00083-2
39. K. Saghiri, I. Daoud, N. Melkemi and F. Mesli, *Chem. Data Collect*., **46**, 101044 (2023); https://doi.org/10.1016/j.cdc.2023.101044
40. T. Alorini, I. Daoud, A.N. Al-Hakimi, F. Alminderej and A.E.A.E. Albadri, *Res. Chem. Intermed*., **49**, 1701 (2023); https://doi.org/10.1007/s11164-022-04922-3
41. R.V. Sakthivel, P. Sankudevan, P. Vennila, G. Venkatesh, S. Kaya and G. Serdaroğlu, *J. Mol. Struct*., **1233**, 130097 (2021); https://doi.org/10.1016/j.molstruc.2021.130097
42. A. Imberty, K.D. Hardman, J.P. Carver and S. Perez, *Glycobiology*, **1**, 631 (1991); https://doi.org/10.1093/glycob/1.6.631